Asymptotic analysis of an anti-plane dynamic problem for a three-layered strongly inhomogeneous laminate

Yağmur Ece Aydın[1], Barış Erbaş[1], Julius Kaplunov[2], and Ludmila Prikazchikova[2]

Abstract
Anti-plane dynamic shear of a strongly inhomogeneous dynamic laminate with traction-free faces is analysed. Two types of contrast are considered, including those for composite structures with stiff thick or thin outer layers. In both cases, the value of the cut-off frequency corresponding to the lowest anti-symmetric vibration mode tends to zero. For this mode the shortened dispersion relations and the associated formulae for displacement and stresses are obtained. The latter motivate the choice of appropriate settings supporting the limiting forms of the original anti-plane problem. The asymptotic equation derived for a three-layered plate with thick faces is valid over the whole low-frequency range, whereas the range of validity of its counterpart for another type of contrast is restricted to a narrow vicinity of the cut-off frequency.

Keywords
asymptotic, contrast, laminate, cut-off, wave

1 Introduction

Layered structures with high contrast in material and geometrical properties of the layers are widely used in modern engineering. Among them, we mention laminated glass and photovoltaic panels [1, 2], smart periodic structures acting as vibration filters [3], microfibre-nanowire hybrid structures in energy scavenging devices [4], and precipitator plates in gas filters [5]. We also note possible applications of high-contrast layered structures in the rapidly growing area of meta-materials, see [6].

Several engineering formulations were developed for modelling high contrast sandwich structures, see [7–11]. Asymptotic considerations on the subject, not emphasizing characteristic peculiarities of dynamic behaviour, were reported in [12] and [13]. In addition, we cite here recent papers [14,15] devoted to homogenization of high-contrast periodic structures. Similarity of the asymptotic techniques for periodic and thin layered structures was addressed in [16].

Dispersion of elastic waves in a three-layered plate was investigated in [17] using an asymptotic approach adapted for dynamic multi-parametric analysis. The conditions for contrast material and

[1]Anadolu University, Department of Mathematics, Yunus Emre Campus, 26470, Eskisehir, Turkey
[2]Keele University, School of Computing and Mathematics, Staffordshire, ST5 5BG, UK

Corresponding author:
Julius Kaplunov, Keele University, School of Computing and Mathematics, Staffordshire, ST5 5BG, UK
Email: j.kaplunov@keele.ac.uk

geometric parameters ensuring the existence of an extra low-frequency shear mode is derived. For four types of contrast inspired by various engineering applications, two-mode polynomial approximations of the 'exact' dispersion relations, involving both the fundamental bending mode and the lowest shear harmonic, were established. The scenarios, for which they are not uniformly valid, are revealed.

In spite of a substantial progress in terms of the qualitative understanding of the effect of contrast on the dynamic response of a layered plate coming from the aforementioned paper [17], asymptotic derivation of the related shortened differential equations of motion from the original 3D vector formulation may still seemingly need a more preliminary insight. This is also due to two distinct kinds of asymptotic behaviour governing bending and shear motions. At the same time, a similar anti-plane shear problem appears to be an excellent framework for developing low-dimensional asymptotic equations within a simpler scalar one-mode setup.

In this paper, we consider anti-symmetric anti-plane shear of a three-layered laminate with traction-free faces. The focus is on two of four types of constrast studied in [17], corresponding to a plate with stiff thick outer layers and soft inner layer (setup (a)) and a conventional sandwich-type plate with thin stiff skins and a soft core (setup (b)). In the absence of contrast, the problem of interest does not support the fundamental mode with a zero cut-off frequency. Under the same condition as in [17] on the contrast parameters, a low-frequency mode arises. For this mode, the shortened forms of the dispersion relation demonstrate different asymptotic behaviours within setups (a) and (b). For setup (a), the shortened dispersion relation is valid over a whole low-frequency domain, whereas for setup (b), the range of validity is restricted to a narrow vicinity of the lowest shear cut-off frequency. Asymptotic low-dimensional equations of motion are obtained for both cases. The near cut-off procedure for setup (b) was earlier widely implemented for analysis of high-frequency long-wave vibrations of plates and shells, e.g. see book [18] and also more recent papers [19–23]. In the last few years it was also developed for vibrations of a cylindrical shell near lowest cut-off frequencies [24, 25].

The governing equations of the problem along with the exact dispersion relation and the parameter settings for setups (a) and (b) are presented in Section 2. The estimation of the lowest shear cut-off frequency and the polynomial dispersion relation, corresponding to long-wave low-frequency limit, are derived in Section 3. The shortened forms of the polynomial dispersion relation in Section 3 are analysed in Section 4 for setups (a) and (b). Asymptotic formulae for displacements and stresses are obtained in Section 5 for both studied cases. Sections 6 and 7 deal with the asymptotic derivation of approximate equations of motion starting from a standard procedure in the theory of thin plates [18] and a near cut-off expansion, respectively.

2 Statement of the problem
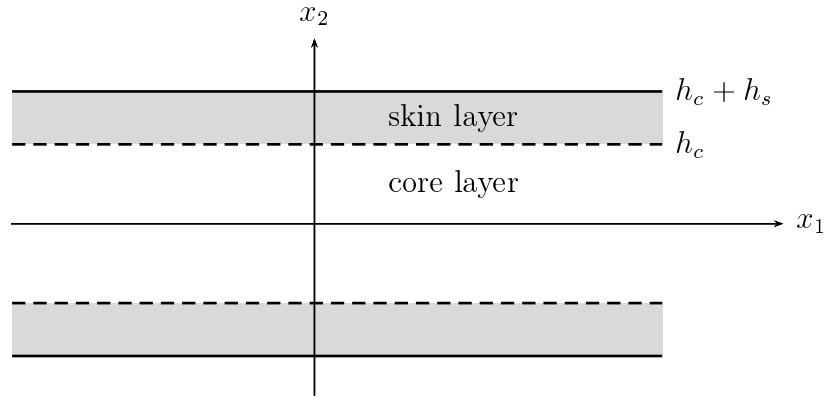
Figure 1. Three-layered laminate

Consider anti-plane shear of a three-layered laminate with the inner layer of thickness $2h_c$ and the outer layers of thickness h_s, see Figure 1. It is assumed that both core and skin layers are isotropic and the whole structure is symmetric about the mid-plane. In Cartesian coordinates x_n, $n = 1, 2, 3$, the equations of motion can be written as

$$\frac{\partial \sigma_{13}^q}{\partial x_1} + \frac{\partial \sigma_{23}^q}{\partial x_2} - \rho_q \frac{\partial^2 u_q}{\partial t^2} = 0, \qquad q = c, s, \tag{1}$$

with

$$\sigma_{i3}^q = \mu_q \frac{\partial u_q}{\partial x_i}, \quad i = 1, 2, \tag{2}$$

where t is time, u_q are out of plane displacements, σ_{i3}^q are shear stresses, μ_q are Lamé parameters, and ρ_q are mass densities. Here and below indices $q = c$ and $q = s$ correspond to core (inner) and skin (outer) layers, respectively. The continuity conditions along interfaces $x_2 = \pm h_c$ are given by

$$\sigma_{23}^c = \sigma_{23}^s \quad \text{and} \quad u_c = u_s. \tag{3}$$

We also impose the traction-free boundary conditions

$$\sigma_{23}^s = 0 \qquad \text{at} \qquad x_2 = \pm(h_c + h_s). \tag{4}$$

Relations (1) can be readily reduced to the wave equations

$$\Delta u_q - \frac{1}{c_{2q}^2} \frac{\partial^2 u_q}{\partial t^2} = 0, \quad q = c, s. \tag{5}$$

with $c_{2q} = \sqrt{\dfrac{\mu_q}{\rho_q}}$.

It can easily be shown that the dispersion relation associated with the formulated problem in case of antisymmetric modes takes the form

$$\mu \alpha_1 \cosh(\alpha_1) \cosh(\alpha_2 h) + \alpha_2 \sinh(\alpha_1) \sinh(\alpha_2 h) = 0, \tag{6}$$

with

$$\alpha_1 = \sqrt{K^2 - \Omega^2}, \qquad \alpha_2 = \sqrt{K^2 - \frac{\mu}{\rho} \Omega^2}, \tag{7}$$

where non-dimensional frequency Ω and wavenumber K have been introduced in the form

$$\Omega = \frac{\omega h_c}{c_{2c}}, \qquad K = k h_c, \tag{8}$$

together with the basic dimensionless problem parameters

$$h = \frac{h_s}{h_c}, \quad \mu = \frac{\mu_c}{\mu_s}, \quad \rho = \frac{\rho_c}{\rho_s}. \tag{9}$$

The related displacements and stresses after separating factor $\exp\{i(kx_1 - \omega t)\}$ are expressed as

$$
\begin{aligned}
u_c &= h_c \frac{\sinh(\alpha_1 \xi_{2c})}{\alpha_1}, \\
\sigma_{13}^c &= i\mu_c K \frac{\sinh(\alpha_1 \xi_{2c})}{\alpha_1}, \\
\sigma_{23}^c &= \mu_c \cosh(\alpha_1 \xi_{2c}),
\end{aligned}
\tag{10}
$$

and

$$
\begin{aligned}
u_s &= h_c \beta \left(\cosh\left[\alpha_2(h\xi_{2s} + 1)\right] - \tanh\left[\alpha_2(h + 1)\right] \sinh\left[\alpha_2(h\xi_{2s} + 1)\right] \right), \\
\sigma_{13}^s &= i\mu_s K \beta \left(\cosh\left[\alpha_2(h\xi_{2s} + 1)\right] - \tanh\left[\alpha_2(h + 1)\right] \sinh\left[\alpha_2(h\xi_{2s} + 1)\right] \right), \\
\sigma_{23}^s &= \mu_s \alpha_2 \beta \left(\sinh\left[\alpha_2(h\xi_{2s} + 1)\right] - \tanh\left[\alpha_2(h + 1)\right] \cosh\left[\alpha_2(h\xi_{2s} + 1)\right] \right),
\end{aligned}
\tag{11}
$$

where

$$\beta = \frac{\sinh \alpha_1}{\alpha_1 \left(\cosh \alpha_2 - \sinh \alpha_2 \tanh[\alpha_2(h + 1)] \right)},$$

together with the scaled variables

$$
\begin{aligned}
\xi_{2c} &= \frac{x_2}{h_c}, \quad 0 \le x_2 \le h_c, \\
\xi_{2s} &= \frac{x_2 - h_c}{h_s}, \quad h_c \le x_2 \le h_c + h_s.
\end{aligned}
\tag{12}
$$

Below we study two setups of the contrast, similar to [17]. They are given by the following asymptotic relations between problem parameters in (9)

$$(a) \ \mu \ll 1, \ h \sim 1, \ \rho \sim \mu, \tag{13}$$

and

$$(b) \ \mu \ll 1, \ h \sim \mu, \ \rho \sim \mu^2, \tag{14}$$

corresponding to a plate with stiff thick skin layers and a soft core and to a traditional sandwich-type structure with thin stiff faces, respectively. In what follows, we demonstrate that the effect of contrast results in low-frequency anti-symmetric vibration modes. At the same time, it is also pretty clear that in absence of contrast, dispersion relation (6) supports high-frequency modes only.

3 Long-wave low-frequency limit: lowest cut-off frequency and polynomial dispersion relation

First, setting $K = 0$ in dispersion relation (6), we have for cut-off frequencies

$$\tan(\Omega) \tan\left(h\sqrt{\frac{\mu}{\rho}}\Omega\right) = \sqrt{\mu\rho}. \tag{15}$$

Over the low frequency range

$$\Omega\left(1 + h\sqrt{\frac{\mu}{\rho}}\right) \ll 1 \tag{16}$$

this predicts the single cut-off frequency

$$\Omega \approx \left(\frac{\rho}{h}\right)^{\frac{1}{2}} \ll 1 \tag{17}$$

provided that

$$\rho \ll h \ll \mu^{-1}. \tag{18}$$

Approximation (17) coincides with that for the lowest shear cut-off frequency for the plane problem in elasticity studied in [17]. In contrast to the latter, the anti-plane problem under consideration does not support the fundamental mode with a zero cut-off frequency.

Let us concentrate on long-wave motions, for which

$$K(1 + h) \ll 1, \tag{19}$$

over low-frequency range (16). To this end, expanding all trigonometric functions in (6) in Taylor series, we derive a polynomial dispersion relation, which can be written as

$$\mu + \gamma_1 K^2 + \gamma_2 K^4 + \gamma_3 K^2 \Omega^2 + \gamma_4 \Omega^2 + \gamma_5 \Omega^4 + \cdots = 0 \tag{20}$$

with

$$\begin{aligned}
\gamma_1 &= \frac{\mu}{2}\left(1 + h^2\right) + h, \\
\gamma_2 &= \frac{\mu}{24}\left(1 + 6h^2 + h^4\right) + \frac{h}{6}(1 + h^2), \\
\gamma_3 &= -\frac{\mu}{12}(1 + 3h^2) - \frac{h}{6} - \frac{\mu h}{12\rho}\left(2 + 3\mu h\right) - \frac{\mu h^3}{12\rho}\left(4 + \mu h\right), \\
\gamma_4 &= -\frac{\mu}{2} - \frac{\mu h}{\rho}\left(1 + \frac{\mu h}{2}\right), \\
\gamma_5 &= \frac{\mu}{24} + \frac{\mu h}{12\rho}(2 + 3\mu h) + \frac{\mu^2 h^3}{24\rho^2}(4 + \mu h).
\end{aligned} \tag{21}$$

Dispersion curves computed from (6) are plotted in Figures 2 and 3 for non-contrast and contrast setups, respectively. In Figure 2, $\mu = 0.232$, $\rho = 3.0$, and $h = 1.0$, while $\mu = 0.014$, $\rho = 0.03$, and $h = 1.0$ in Figure 3. In Figure 3, the lowest cut-off frequency $\Omega = 0.17$, and formula (17) gives the same value. As might be expected, the cut-off frequencies are not observed over the low-frequency range in the non-contrast case, see Figure 2.
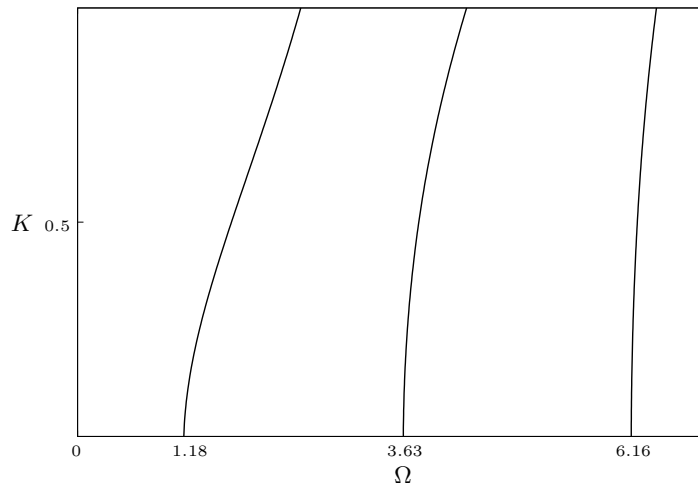
Figure 2. Dispersion curves for laminate with $\mu = 0.232$, $\rho = 3.0$, and $h = 1.0$.
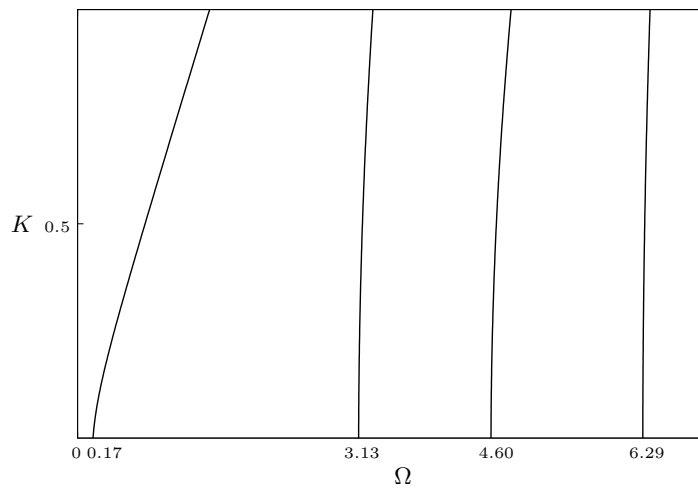
Figure 3. Dispersion curves for laminate with $\mu = 0.014$, $\rho = 0.03$, and $h = 1.0$.

In the next section, we further simplify asymptotic dispersion relation (20) by specifying coefficients γ_j for two chosen scenarios, (13) and (14).

4 Shortened polynomial dispersion relations

For parameter setup (a), see (13), we readily deduce from formulae (21)

$$\gamma_1 \sim \gamma_2 \sim \gamma_3 \sim \gamma_4 \sim \gamma_5 \sim 1 \tag{22}$$

At leading order

$$\gamma_1 = h$$
$$\gamma_2 = \frac{h(1+h^2)}{6}$$
$$\gamma_3 = -\frac{h}{6\rho_\mu}\left(\rho_\mu + 1 + 2h^2\right) \tag{23}$$
$$\gamma_4 = -\frac{h}{\rho_\mu}$$
$$\gamma_5 = \frac{h}{6\rho_\mu}\left(1 + \frac{h^2}{\rho_\mu}\right)$$

where $\rho_\mu = \dfrac{\rho}{\mu} \sim 1$. As a result, we arrive at the shortened dispersion relation

$$\frac{\mu}{h} + K^2 - \frac{1}{\rho_\mu}\Omega^2 = 0. \tag{24}$$

Next, let us scale in (24) the dimensionless frequency and wavenumber by

$$\Omega^2 = \mu^\alpha \Omega_*^2 \quad \text{and} \quad K^2 = \mu^\alpha K_*^2, \tag{25}$$

where $\Omega_* \sim K_* \sim 1$ and $0 < \alpha \le 1$. This interval of parameter α covers the whole long-wave low-frequency band, which is now given by $\Omega \ll 1$, and $K \ll 1$, see (16) and (19).

Dispersion relation (24) expressed in Ω_* and K_* becomes

$$\Omega_*^2 = \rho_\mu\left(K_*^2 + \frac{\mu^{1-\alpha}}{h}\right). \tag{26}$$

At $\alpha < 1$ we have $\Omega_* \sim \sqrt{\rho_\mu}K_*$ or $\omega \sim c_{2s}k$, corresponding to the short-wave limit for stiffer skin layers.
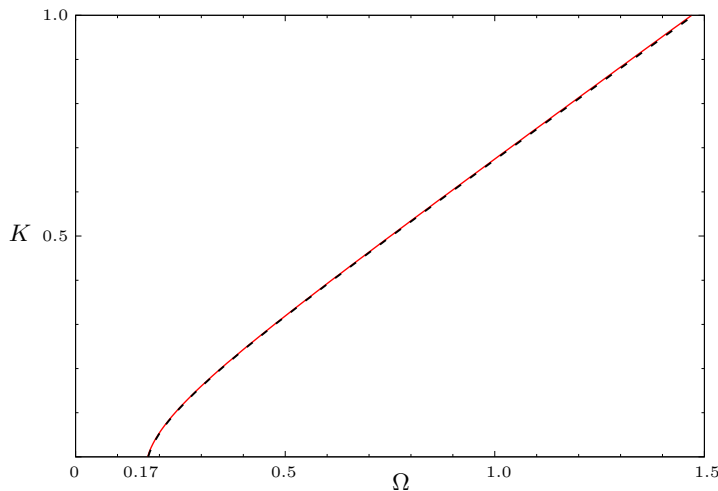
Figure 4. Lowest dispersion branch corresponding to transcendental equation (6) (red solid line) and shortened formula (24) (black dashed line)
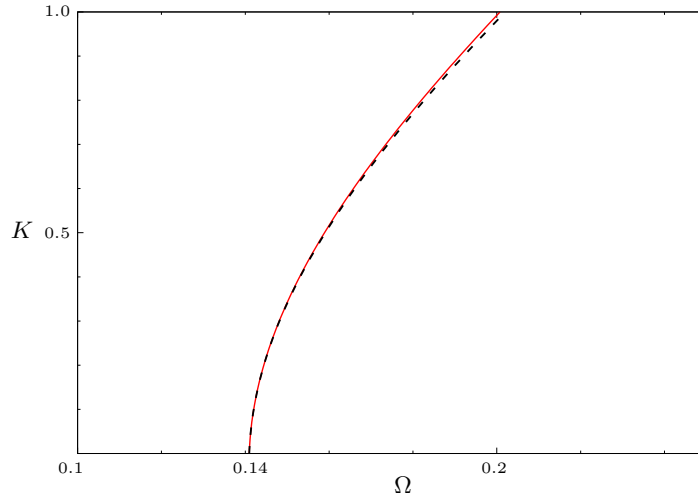
Figure 5. Lowest dispersion branch corresponding to transcendental equation (6) (red solid line) and shortened formula (34) (black dashed line)

Figure 4 displays dispersion curves by shortened formula (24) and original transcendental equation (6) for the same set of parameters as in Figure 3. A good agreement over a broad frequency range is observed.

For setup (b), see (14), we obtain from (21)

$$\gamma_1 \sim \gamma_2 \sim \mu \quad \text{and} \quad \gamma_3 \sim \gamma_4 \sim \gamma_5 \sim 1. \tag{27}$$

This time, in addition to the leading order expansion for coefficients γ_j, $j \neq 4$, we also need a two-term expansion for coefficient γ_4. Thus, we have

$$
\begin{aligned}
\gamma_1 =& \mu \left(\frac{1}{2} + h_\mu \right) \\
\gamma_2 =& \frac{\mu}{6} \left(\frac{1}{4} + h_\mu \right) \\
\gamma_3 =& -\frac{h_\mu}{6\rho_\mu} \\
\gamma_4 =& -\frac{h_\mu}{\rho_\mu} - \frac{\mu}{2} \\
\gamma_5 =& \frac{h_\mu}{6\rho_\mu}.
\end{aligned}
\tag{28}
$$

where $\rho_\mu = \dfrac{\rho}{\mu^2} \sim 1$ and $h_\mu = \dfrac{h}{\mu} \sim 1$. The sought for dispersion relation becomes

$$\mu + \mu \left(\frac{1}{2} + h_\mu \right) K^2 - \frac{h_\mu}{6\rho_\mu} K^2 \Omega^2 - \left(\frac{\mu}{2} + \frac{h_\mu}{\rho_\mu} \right) \Omega^2 + \frac{h_\mu}{6\rho_\mu} \Omega^4 = 0. \tag{29}$$

Now, let us normalize wavenumber and frequency by

$$K^2 = \mu K_*^2 \quad \text{and} \quad \Omega^2 = \mu \Omega_*^2, \tag{30}$$

having from (29)

$$1 + \mu \left(\frac{1}{2} + h_\mu \right) K_*^2 - \mu \frac{h_\mu}{6\rho_\mu} K_*^2 \Omega_*^2 - \left(\frac{\mu}{2} + \frac{h_\mu}{\rho_\mu} \right) \Omega_*^2 + \mu \frac{h_\mu}{6\rho_\mu} \Omega_*^4 = 0, \tag{31}$$

and adapt a near cut-off asymptotic expansion in the form

$$\Omega_*^2 = \Omega_0^2 + \mu \Omega_1^2 + \cdots \tag{32}$$

On substituting the latter into (31), we find

$$\Omega_0^2 = \frac{\rho_\mu}{h_\mu} \quad \text{and} \quad \Omega_1^2 = \frac{\rho_\mu}{h_\mu} \left(\frac{1}{3} + h_\mu \right) K_*^2 - \frac{1}{3} \frac{\rho_\mu^2}{h_\mu^2}, \tag{33}$$

leading to the optimal shortened dispersion relation

$$\left(h_\mu + \frac{1}{3} \right) K^2 - \frac{1}{\mu} \frac{h_\mu}{\rho_\mu} \Omega^2 + \left(1 - \frac{\mu \rho_\mu}{3 h_\mu} \right) = 0. \tag{34}$$

In contrast to the previous case, it is valid only over a narrow vicinity of the cut-off frequency, as also illustrated by Figure 5 plotted for $\mu = 0.014$, $\rho = 0.03$, and $h = 1.0$. Indeed, the dispersion curves in this figure corresponding to (6) and (34) rapidly approach the bound of long-wave region.

5 Asymptotic formulae for displacements and stresses

On inserting $K^2 = \mu K_*^2$ and $\Omega^2 = \mu \Omega_*^2$ into formulae (10) and (11) we have for leading order displacements and stresses within setup (a), see (13),

$$\begin{aligned} u_c &= h_c \xi_{2c}, \\ \sigma_{13}^c &= i\mu_c \sqrt{\mu} \, K_* \xi_{2c}, \\ \sigma_{23}^c &= \mu_c, \end{aligned} \tag{35}$$

and

$$\begin{aligned} u_s &= h_c, \\ \sigma_{13}^s &= i\mu_s \sqrt{\mu} K_*, \\ \sigma_{23}^s &= \mu_c h \left(K_*^2 - \frac{\Omega_*^2}{\rho_\mu} \right) (\xi_{2s} - 1). \end{aligned} \tag{36}$$

For setup (b), see (14), these relations hold true, except for the last formula in (36), which now has to be replaced by

$$\sigma_{23}^s = \mu_c \frac{h_\mu \Omega_*^2}{\rho_\mu} (1 - \xi_{2s}). \tag{37}$$

As a consequence, we obtain for both setups

$$\frac{u_q}{h_c} \sim \frac{\sigma_{23}^q}{\mu_c} \sim \frac{\sigma_{13}^q}{\mu_q \sqrt{\mu}}, \tag{38}$$

where, as above, $q = c, s$.

The normalized displacements and one of the stresses for case (a) are presented in Figures 6 and 7. In these figures $\xi_2 = \xi_{2c}$, $u = \dfrac{u_c}{h_c}$, and $\sigma_{23} = \dfrac{\sigma_{23}^c}{\mu_c}$, $(0 < \xi_2 \leq 1)$ or $\xi_2 = 1 + \xi_{2s}$, $u = \dfrac{u_s}{h_c}$, and $\sigma_{23} = \dfrac{\sigma_{23}^s}{\mu_c}$, $(1 < \xi_2 \leq 2)$, see formula (12). The problem parameters here are the same as in figures (3) and (4). Numerical results obtain from asymptotic formula (35), and (36) and exact solution (10), and (11) are compared with each other. In spite of drastical difference between two studied settings (13) and (14), including the behaviour of parameter h expressing the ratio of thicknesses, analogous graphs for case(b) plotted in scaled coordinate ξ_2 appear to have virtually the same form.
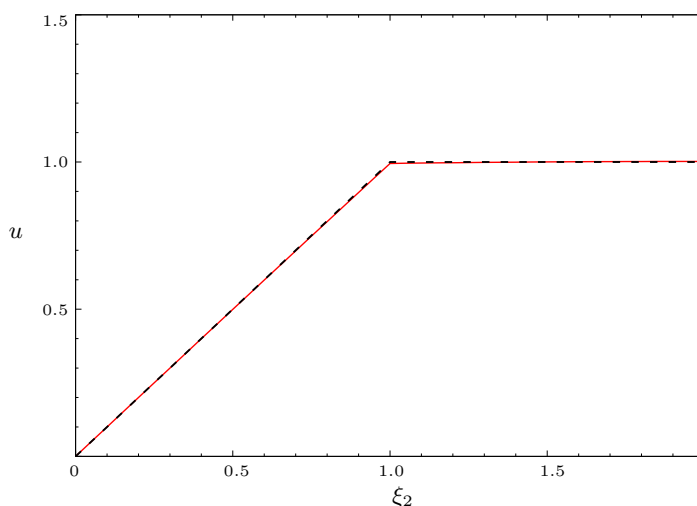
Figure 6. Normalized displacement u computed from exact relations (10) and (11) (red solid line) and asypmtotic formulae (35) and(36) (black dashed line)

.
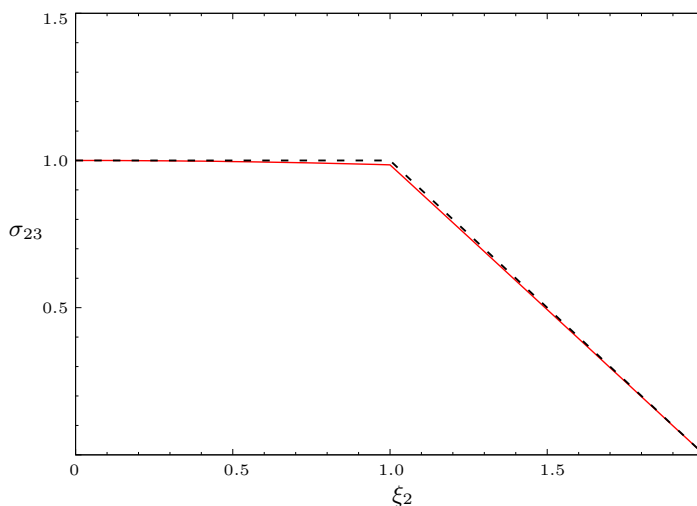
Figure 7. Normalized stresses σ_{23} computed from exact relations (10) and (11) (red solid line) and asypmtotic formulae (35) and(36) (black dashed line)

6 Long-wave low-frequency approximation of equations of motions

Let us return back to setup (a) again assuming the problem parameters to be related to each other by formulae (13). First, scale longitudinal coordinate and time by

$$x_1 = \frac{h_c}{\sqrt{\mu}}\xi_1 \quad \text{and} \quad t = \frac{h_c}{c_{2c}\sqrt{\mu}}\tau,$$
(39)

using transformations (12) for transverse variable x_2. Also, motivated by asymptotic formulae (35) and (36), we normalise displacement and stresses as

$$u^q = h_c v^q, \quad \sigma_{13}^q = \mu_q\sqrt{\mu}S_{13}^q, \quad \sigma_{23}^q = \mu_c S_{23}^q, \quad q = c, s.$$
(40)

with all dimensionless quantities assumed to be of order unity. Then, we insert (39) and (40) as well as (12) into governing equations (1)–(4) in Section 2 to obtain for the core and skin layers, respectively,

$$\mu\frac{\partial S_{13}^c}{\partial \xi_1} + \frac{\partial S_{23}^c}{\partial \xi_{2c}} - \mu\frac{\partial^2 v^c}{\partial \tau^2} = 0.$$
(41)
$$S_{13}^c = \frac{\partial v^c}{\partial \xi_1}, \quad S_{23}^c = \frac{\partial v^c}{\partial \xi_{2c}}$$

and

$$\frac{\partial S_{13}^s}{\partial \xi_1} + \frac{1}{h}\frac{\partial S_{23}^s}{\partial \xi_{2s}} - \frac{1}{\rho_\mu}\frac{\partial^2 v^s}{\partial \tau^2} = 0,$$
(42)
$$S_{13}^s = \frac{\partial v^s}{\partial \xi_1}, \quad \mu h S_{23}^s = \frac{\partial v^s}{\partial \xi_{2s}},$$

where $\rho_\mu = \dfrac{\rho}{\mu} \sim 1$. In this case the continuity and boundary conditions become

$$v^c\big|_{\xi_{2c}=1} = v^s\big|_{\xi_{2s}=0}$$
$$S_{23}^c\big|_{\xi_{2c}=1} = S_{23}^s\big|_{\xi_{2s}=0}$$
(43)

and

$$S_{23}^s\big|_{\xi_{2s}=1} = 0.$$
(44)

Now, expand displacements and stresses into asymptotic series as

$$v^q = v_0^q + \mu v_1^q + \cdots,$$
(45)
$$S_{j3}^q = S_{j3,0}^q + \mu S_{j3,1}^q + \cdots, \quad q = c, s \quad \text{and} \quad j = 1, 2.$$

On substituting these into formulae (41)- (44), we arrive at leading order at

$$S_{13,0}^c = \frac{\partial v_0^c}{\partial \xi_1}, \quad \frac{\partial S_{23,0}^c}{\partial \xi_{2c}} = 0, \quad S_{23,0}^c = \frac{\partial v_0^c}{\partial \xi_{2c}},$$
(46)

and

$$\frac{\partial S_{13,0}^s}{\partial \xi_1} + \frac{1}{h}\frac{\partial S_{23,0}^s}{\partial \xi_{2s}} - \frac{1}{\rho_\mu}\frac{\partial^2 v_0^s}{\partial \tau^2} = 0,$$
(47)

$$S^s_{13,0} = \frac{\partial v^s_0}{\partial \xi_1}, \quad \frac{\partial v^s_0}{\partial \xi_{2s}} = 0 \tag{48}$$

with

$$\left. v^c_0 \right|_{\xi_{2c}=1} = \left. v^s_0 \right|_{\xi_{2s}=0}$$
$$\left. S^c_{23,0} \right|_{\xi_{2c}=1} = \left. S^s_{23,0} \right|_{\xi_{2s}=0} \tag{49}$$

and

$$\left. S^s_{23} \right|_{\xi_{2s}=1} = 0 \tag{50}$$

Next, we obtain from the second equation in (48)

$$v^s_0 = w(\xi_1, \tau). \tag{51}$$

The rest of the quantities in (46)–(50) are expressed in terms of w as

$$S^c_{13,0} = \xi_{2c}\frac{\partial w}{\partial \xi_1}, \qquad S^c_{23,0} = w, \qquad v^c_0 = \xi_{2c}w, \tag{52}$$

$$S^s_{13,0} = \frac{\partial w}{\partial \xi_1}, \qquad S^s_{23,0} = w(1 - \xi_{2s}), \tag{53}$$

with w satisfying the 1D equation

$$\frac{\partial^2 w}{\partial \xi_1^2} - \frac{1}{\rho_\mu}\frac{\partial^2 w}{\partial \tau^2} - \frac{1}{h}w = 0, \tag{54}$$

which may be presented in the original variables as

$$\frac{\partial^2 u_s}{\partial x_1^2} - \frac{\rho_s}{\mu_s}\frac{\partial^2 u_s}{\partial t^2} - \frac{\mu_c}{\mu_s h_c h_s}u_s = 0, \tag{55}$$

where $u_s(x_1, t) \approx w(x_1, t)$.

Let us insert ansatz $u_s = \exp\{i(kx_1 - wt)\}$ into the last equation. As a result, we have the dispersion relation

$$k^2 - \frac{\rho_s}{\mu_s}\omega^2 + \frac{\mu_c}{\mu_s h_c h_s} = 0, \tag{56}$$

coinciding with (24) in Section 4.

7 Near cut-off approximation of equations of motion

For parameter setup (b), see (14), we may use the same scaling of the independent variables and time (12), and (39) and also start from the asymptotic behaviour of displacements and stresses predicted by (40). Then, the original relations in Section 2 become

$$\mu\frac{\partial S^c_{13}}{\partial \xi_1} + \frac{\partial S^c_{23}}{\partial \xi_{2c}} + \mu\Omega^2_0 v^c - \mu^2 L(v^c) = 0, \tag{57}$$

$$S^c_{13} = \frac{\partial v^c}{\partial \xi_1}, \quad S^c_{23} = \frac{\partial v^c}{\partial \xi_{2c}}$$

and

$$\mu \frac{\partial S_{13}^s}{\partial \xi_1} + \frac{1}{h_\mu} \frac{\partial S_{23}^s}{\partial \xi_{2s}} + \frac{1}{\rho_\mu} \Omega_0^2 v^s - \frac{\mu}{\rho_\mu} L(v^s) = 0, \tag{58}$$

$$S_{13}^s = \frac{\partial v^s}{\partial \xi_1}, \quad \mu^2 h_\mu S_{23}^s = \frac{\partial v^s}{\partial \xi_{2s}}$$

with continuity and boundary conditions (43) and (44), where Ω_0 is a frequency to be found, $h_\mu = \dfrac{h}{\mu} \sim 1$, $\rho_\mu = \dfrac{\rho}{\mu^2} \sim 1$, and

$$L(v^q) = \frac{1}{\mu} \left(\Omega_0^2 v^q + \frac{\partial^2 v^q}{\partial \tau^2} \right), \quad q = c, s. \tag{59}$$

This operator is introduced for taking into account a small deviation from time-harmonic vibrations with frequency Ω_0. This setup appears to be a natural generalisation of near cut-off expansion (32) of dispersion relation (31). Before, near cut-off expansions were widely expoited for analysing high-frequency long-wave vibrations of homogenous plates and shells, e.g. see [18].

On substituting asymptotic expansion (45) into the formulae above, we obtain at leading order

$$\frac{\partial S_{23,0}^c}{\partial \xi_{2c}} = 0, \quad S_{23,0}^c = \frac{\partial v_0^c}{\partial \xi_{2c}}, \quad S_{13,0}^c = \frac{\partial v_0^c}{\partial \xi_1}$$

$$\frac{1}{h_\mu} \frac{\partial S_{23,0}^s}{\partial \xi_{2s}} + \frac{1}{\rho_\mu} \Omega_0^2 v_0^s = 0$$

$$S_{13,0}^s = \frac{\partial v_0^s}{\partial \xi_1}, \quad \frac{\partial v_0^s}{\partial \xi_{2s}} = 0 \tag{60}$$

with (49) and (50).

Next, we deduce from the first and last equations in (60), respectively,

$$S_{23,0}^c = p_1(\xi_1, \tau) \quad \text{and} \quad v_0^s = w_2(\xi_1, \tau) \tag{61}$$

and also observe that frequency Ω_0 coincides with the leading order term in near cut-off asymptotic expansion (31). As a result, we have

$$S_{13,0}^c = \xi_{2c} \frac{\partial w_2}{\partial \xi_1}, \quad v_0^c = \xi_{2c} p_1, \tag{62}$$

and

$$S_{13,0}^s = \frac{\partial w_2}{\partial \xi_1}, \quad S_{23,0}^s = w_2(1 - \xi_{2s}). \tag{63}$$

In contrast to the consideration in the previous section, the adapted near cut-off scheme suggests to proceed to the next asymptotic order. Thus, we arrive at the equations

$$\frac{\partial S_{13,0}^c}{\partial \xi_1} + \frac{\partial S_{23,1}^c}{\partial \xi_{2c}} + \frac{\rho_\mu}{h_\mu} v_0^c = 0 \tag{64}$$

$$S_{13,1}^c = \frac{\partial v_1^c}{\partial \xi_1}, \quad S_{23,1}^c = \frac{\partial v_1^c}{\partial \xi_{2c}}$$

and

$$\frac{\partial S^s_{13,0}}{\partial \xi_1} + \frac{1}{h_\mu}\frac{\partial S^s_{23,1}}{\partial \xi_{2s}} + \frac{v^s_1}{h_\mu} - \frac{L(w_2)}{\rho_\mu} = 0 \tag{65}$$

$$S^s_{13,1} = \frac{\partial v^s_1}{\partial \xi_1}, \quad \frac{\partial v^s_1}{\partial \xi_{2s}} = 0$$

with

$$v^c_1\big|_{\xi_{2c}=1} = v^s_1\big|_{\xi_{2s}=0} \tag{66}$$

$$S^c_{23,1}\big|_{\xi_{2c}=1} = S^s_{23,1}\big|_{\xi_{2s}=0}$$

and

$$S^s_{23,1}\big|_{\xi_{2s}=1} = 0. \tag{67}$$

On integrating them across the thickness and taking into account (62) and (63), we establish that $p_1 = w_2$ along with the expressions

$$
\begin{aligned}
S^c_{13,1} =& \xi_1 \left(\left(\frac{\xi_{2c}}{2} - \frac{\xi^3_{2c}}{6} \right) \left(\frac{\partial^3 w_2}{\partial \xi^3_1} + \frac{\rho_\mu}{h_\mu}\frac{\partial w_2}{\partial \xi_1} \right) - \xi_{2c}h_\mu \left(\frac{L(w_2)}{\rho_\mu} - \frac{\partial^2 w_2}{\partial \xi^2_1} - \frac{w_3}{h_\mu} \right) \right) \\
S^c_{23,1} =& \left(\frac{1}{2} - \frac{\xi^2_{2c}}{2} \right) \left(\frac{\partial^2 w_2}{\partial \xi^2_1} + \frac{\rho_\mu}{h_\mu}w_2 \right) - h_\mu \left(\frac{L(w_2)}{\rho_\mu} - \frac{\partial^2 w_2}{\partial \xi^2_1} - \frac{w_3}{h_\mu} \right) \\
v^c_1 =& \left(\frac{\xi_{2c}}{2} - \frac{\xi^3_{2c}}{6} \right) \left(\frac{\partial^2 w_2}{\partial \xi^2_1} + \frac{\rho_\mu}{h_\mu}w_2 \right) - \xi_{2c}h_\mu \left(\frac{L(w_2)}{\rho_\mu} - \frac{\partial^2 w_2}{\partial \xi^2_1} - \frac{w_3}{h_\mu} \right) \\
S^s_{13,1} =& \frac{\partial w_3}{\partial \xi_1} \\
S^s_{23,1} =& h_\mu(\xi_{2s} - 1) \left(\frac{L(w_2)}{\rho_\mu} - \frac{\partial^2 w_2}{\partial \xi^2_1} - \frac{w_3}{h_\mu} \right) \\
v^s_1 =& w_3(\xi_1, \tau),
\end{aligned}
\tag{68}
$$

where the sought for function w_2 satisfies the 1D equation

$$\left(h_\mu + \frac{1}{3} \right) \frac{\partial^2 w_2}{\partial \xi^2_1} + \frac{\rho_\mu}{3h_\mu}w_2 - \frac{h_\mu}{\rho_\mu}L(w_2) = 0, \tag{69}$$

which can be transformed to

$$\left(\frac{h_s\mu_s}{h_c\mu_c} + \frac{1}{3} \right) \frac{\partial^2 u_s}{\partial x^2_1} - \frac{h_s\rho_s}{h_c\mu_c}\frac{\partial^2 u_s}{\partial t^2} - \frac{1}{h^2_c}\left(1 - \frac{h_c\rho_c}{3h_s\rho_s} \right) u_s = 0 \tag{70}$$

with $u_s(x_1, t) \approx w_2(x_1, t)$.

As might be expected, the associated dispersion relation

$$\left(\frac{h_s\mu_s}{h_c\mu_c} + \frac{1}{3} \right) k^2 - \frac{h_s\rho_s}{h_c\mu_c}\omega^2 + \frac{1}{h^2_c}\left(1 - \frac{h_c\rho_c}{3h_s\rho_s} \right) = 0 \tag{71}$$

is identical to (34).

Concluding Remarks

Asymptotic equations of motion (55) and (70) are established for two distinct setups of contrast parameters. The former is applicable over the whole low-frequency range, while the second one is valid only over a narrow vicinity of the lowest cut-off frequency. Dispersion relations (56) and (71) following from these equations agree with the numerically tested shortened forms (24) and (34) of exact dispersion relation (6), see Figures 4 and 5.

For the sake of simplicity, the adapted near cut-off asymptotic routine in Section 7 does not fully rely on the method of multiple scales as it has been done in [26] and [27]. The obtained results may be extended to similar anti-plane problems for asymmetric multi-layered structures as well as to more sophisticated plane and 3D problems. We also remark that proper formulation of the boundary conditions for systems with a small but nonzero cut-off frequency may require implementation of the low-frequency decay conditions [28], generalising the classical St. Venant principle for an elastic semi-infinite strip.

Acknowledgements

References

[1] Aßmus M, Naumenko K and Altenbach H. Mechanical behaviour of photovoltaic composite structures: Influence of geometric dimensions and material properties on the eigenfrequencies of mechanical vibrations. *Composites Communications* 2017; 6: 59–62.

[2] Ivanov IV. Analysis, modelling, and optimization of laminated glasses as plane beam. *International Journal of Solids and Structures* 2006; 43(22): 6887–6907.

[3] Ruzzene M and Baz A. Attenuation and localization of wave propagation in periodic rods using shape memory inserts. *Smart materials and Structures* 2000; 9(6): 805.

[4] Qin Y, Wang X and Wang ZL. Microfibre–nanowire hybrid structure for energy scavenging. *Nature* 2008; 451(7180): 809–813.

[5] Lee P and Chang N. Harmonic waves in elastic sandwich plates. *Journal of Elasticity* 1979; 9(1): 51–69.

[6] Martin TP, Layman CN, Moore KM et al. Elastic shells with high-contrast material properties as acoustic metamaterial components. *Physical Review B* 2012; 85(16): 161103.

[7] Altenbach H, Eremeyev VA and Naumenko K. On the use of the first order shear deformation plate theory for the analysis of three-layer plates with thin soft core layer. *ZAMM-Journal of Applied Mathematics and Mechanics/Zeitschrift für Angewandte Mathematik und Mechanik* 2015; 95(10): 1004–1011.

[8] Aşık MZ and Tezcan S. A mathematical model for the behavior of laminated glass beams. *Computers & Structures* 2005; 83(21): 1742–1753.

[9] Aßmus M, Naumenko K and Altenbach H. A multiscale projection approach for the coupled global–local structural analysis of photovoltaic modules. *Composite Structures* 2016; 158: 340–358.

[10] Carrera E. Historical review of zig-zag theories for multilayered plates and shells. *Applied mechanics reviews* 2003; 56(3): 287–308.

[11] Sayyad AS and Ghugal YM. Bending, buckling and free vibration of laminated composite and sandwich beams: A critical review of literature. *Composite Structures* 2017; .

[12] Berdichevsky VL. An asymptotic theory of sandwich plates. *International Journal of Engineering Science* 2010; 48(3): 383–404.

[13] Tovstik PE and Tovstik TP. Generalized Timoshenko-Reissner models for beams and plates, strongly heterogeneous in the thickness direction. *ZAMM-Journal of Applied Mathematics and Mechanics/Zeitschrift für Angewandte Mathematik und Mechanik* 2016; DOI:10.1002/zamm.201600052.

[14] Cherdantsev M, Cherednichenko K and Cooper S. Extreme localisation of eigenfunctions to one-dimensional high-contrast periodic problems with a defect. *arXiv preprint arXiv* 2017; 1702.03538.

[15] Kaplunov J and Nobili A. Multi-parametric analysis of strongly inhomogeneous periodic waveguides with internal cut-off frequencies. *Mathematical Methods in the Applied Sciences* 2017; 40(9): 3381–3392. DOI:10.1002/mma.3900.

[16] Craster R, Joseph L and Kaplunov J. Long-wave asymptotic theories: the connection between functionally graded waveguides and periodic media. *Wave Motion* 2014; 51(4): 581–588.

[17] Kaplunov J, Prikazchikov D and Prikazchikova L. Dispersion of elastic waves in a strongly inhomogeneous three-layered plate. *International Journal of Solids and Structures* 2017; 113: 169–179.

[18] Kaplunov JD, Kossovich LY and Nolde EV. *Dynamics of thin walled elastic bodies*. Academic Press, 1998.

[19] Kaplunov J, Kossovich L and Rogerson G. Direct asymptotic integration of the equations of transversely isotropic elasticity for a plate near cut-off frequencies. *The Quarterly Journal of Mechanics and Applied Mathematics* 2000; 53(2): 323–341.

[20] Kaplunov J and Nolde E. Long-wave vibrations of a nearly incompressible isotropic plate with fixed faces. *The Quarterly Journal of Mechanics and Applied Mathematics* 2002; 55(3): 345–356.

[21] Nolde E and Rogerson G. Long wave asymptotic integration of the governing equations for a pre-stressed incompressible elastic layer with fixed faces. *Wave motion* 2002; 36(3): 287–304.

[22] Gridin D, Craster RV and Adamou AT. Trapped modes in curved elastic plates. *Proceedings of the Royal Society of London A: Mathematical, Physical and Engineering Sciences* 2005; 461(2056): 1181–1197.

[23] Rogerson GA and Prikazchikova LA. Generalisations of long wave theories for pre-stressed compressible elastic plates. *International Journal of Non-Linear Mechanics* 2009; 44(5): 520–529.

[24] Kaplunov J, Manevitch L and Smirnov V. Vibrations of an elastic cylindrical shell near the lowest cut-off frequency. *Proc R Soc A* 2016; 472(2189): 20150753.

[25] Kaplunov J and Nobili A. A robust approach for analysing dispersion of elastic waves in an orthotropic cylindrical shell. *Journal of Sound and Vibration* 2017; 401: 23–35.

[26] Nolde E. Qualitative analysis of initial-value problems for a thin elastic strip. *IMA journal of applied mathematics* 2007; 72(3): 348–375.

[27] Andrianov I, Kaplunov J, Kudaibergenov A et al. The effect of a weak nonlinearity on the lowest cut-off frequencies of a cylindrical shell. *Zeitschrift für angewandte Mathematik und Physik* 2018; 69(1): 7.

[28] Babenkova E and Kaplunov J. Low-frequency decay conditions for a semi-infinite elastic strip. *Proceedings of the Royal Society of London A: Mathematical, Physical and Engineering Sciences* 2004; 460(2048): 2153–2169.